

Single Hydrophone Source Localization

Sérgio M. Jesus, *Associate Member, IEEE*, Michael B. Porter, Yann Stéphan, Xavier Démoulin, Orlando C. Rodríguez, and Emanuel M. M. Ferreira Coelho

Abstract—The method presented in this paper assumes that the received signal is a linear combination of delayed and attenuated uncorrelated replicas of the source emitted waveform. The set of delays and attenuations, together with the channel environmental conditions, provide sufficient information for determining the source location. If the transmission channel is assumed known, the source location can be estimated by matching the data with the acoustic field predicted by the model conditioned on the estimated delay set. This paper presents alternative techniques that do not directly attempt to estimate time delays from the data but, instead, estimate the subspace spanned by the delayed source signal paths. Source localization is then done using a family of measures of the distance between that subspace and the subspace spanned by the replicas provided by the model. Results obtained on the INTIMATE'96 data set, in a shallow-water acoustic channel off the coast of Portugal, show that a sound source emitting a 300–800-Hz LFM sweep could effectively be localized in range or depth over an entire day.

Index Terms—Broad-band, shallow water, source localization, subspace methods.

I. INTRODUCTION

THE AIM OF single-hydrophone broad-band source localization is to provide a range/depth localization approach for coherently using the information contained in the time series received by a single hydrophone.

Classical matched-field processing (MFP) methods mostly use vertical or horizontal hydrophone arrays with significant apertures in order to obtain sufficient source location spatial discrimination. The reader is referred to the pioneering work of Hinich [1] and Bucker [2] and to Baggeroer *et al.* [3] and references therein for a full overview of the classical work done in MFP. Although many studies used MFP with single-frequency data (tones), some do combine information at different frequencies. Both incoherent and coherent forms have been studied providing what are effectively broad-band MFP (BBMFP) estimators [4]–[6].

Manuscript received July 31, 1998; revised June 21, 1999, and December 15, 1999. This work was supported in part by PRAXIS, FCT, Portugal, and by the Office of Naval Research.

S. M. Jesus and O. C. Rodríguez are with the UCEH—Universidade do Algarve, PT-8000 Faro, Portugal.

M. B. Porter is with the Center for Communications and Signal Processing Research and Department of Mathematical Sciences, New Jersey Institute of Technology, Newark, NJ 07102 USA.

Y. Stéphan and X. Démoulin are with the CMO-Service Hydrographique et Oceanographique de la Marine, F-29275 Brest Cedex, France.

E. M. M. Ferreira Coelho is with the Instituto Hidrográfico, PT-1296 Lisboa, Portugal.

Publisher Item Identifier S 0364-9059(00)05936-7.

Source localization in the time domain was first clearly suggested by Clay [7]¹ who used a time reversal of the channel impulse response to reduce transmission distortion and (in simulation) localize a source. Li *et al.* [9] used the same technique for localizing a source in a laboratory waveguide using air as the medium of propagation. Single-hydrophone localization, in particular, was studied by Frazer [10], who introduced several Clay-like estimators and tested them on simulated data. In 1992, Miller *et al.* [11] showed, using computer simulations, that it is possible to localize short-duration acoustic signals in a realistic range-dependent environment, while the same method was applied for range and bearing estimation using bottom moored sensors in [12]. Time-domain source localization was actually achieved by Brienzo *et al.* [13] using data received on a vertical array in a deep-water area on the Monterey fan. In this case, a generalized conventional beamformer was used for recombining the received data in the time domain (matched-filter), and then between sensors in the space domain (beamformer).

In shallow water, arrival time estimation is in many practical situations compromised due to the low signal-to-noise ratio (SNR) and/or to the difficulty in resolving individual paths [14]. Furthermore, because of such factors as bottom interaction and ocean variability, shallow water presents many challenges for accurate acoustic modeling. Nevertheless, in a more recent study, it has been demonstrated that, with suitably robust processors, received and model-predicted waveforms could be correlated at a single array sensor yielding practical schemes for source tracking [15], [16]. In this case, the lack of spatial information was “compensated” by coherent broad-band processing.

Difficulties associated with single-hydrophone localization are obviously related with the lack of spatial diversity. Thus, a key point of interest is to understand the degree to which spatial aperture can be compensated for using broad-band information. The method proposed in this paper goes along the lines of those being used in ocean tomography, where the features of interest for ocean characterization are the time delays associated with the different acoustic paths (or rays) [17]. Our approach does not directly attempt to estimate time delays from the data but, instead, searches for the source location for which the time delay set maximizes a mean least squares criteria. In that sense, it gives a mean least squares solution constrained to the given acoustic model.

Making the further assumption that there are features (clusters of acoustic arrivals) that are decorrelated allows us to extend this approach to signal–noise subspace splitting. In that case, estimating the source location is equivalent to measuring the dis-

¹However, source localization feasibility had been mentioned ten years earlier by Parvulescu [8].

tance between the estimated signal subspace and the subspace spanned by the delayed source signal paths given by the acoustic model. Such subspace-based distance measures are shown to yield good source location estimates on real data.

This paper is organized as follows. Section II presents the linear data model and the assumptions that underline the methods being developed. Section III presents the classical time-delay estimation (TDE) problem. Section IV extends TDE methods to source localization by including the environmental information. The resulting algorithm is then tested, with simulated data, in Section V. Section VI shows the results obtained on a data set recorded in a shallow-water area off the west coast of Portugal, during the INTIMATE'96 experiment in June 1996. Finally, in Section VII, we discuss the results and draw some conclusions.

II. LINEAR DATA MODEL

According to the linear data model, the received acoustic signal due to a source at location $\theta_s = (r_s, z_s)$ is given by

$$y_n(t, \theta_s) = z_n(t, \theta_s) + \epsilon_n(t) \quad (1)$$

where ϵ is the noise sequence, assumed spatially and temporally white, zero-mean and uncorrelated with the signal, $t = 1, \dots, T$ is the discrete-time index within each n -index time snapshot, and z is the noise-free signal given by

$$z_n(t, \theta_s) = p_n(t, \theta_s) * s_0(t). \quad (2)$$

Here, s_0 is the source-emitted waveform and p is the channel impulse response. Under the assumption that the medium between the source and the receiver behaves as a multiple time-delay attenuation channel, its impulse response can be written

$$p_n(t, \theta_s) = \sum_{m=1}^M a_{n,m}(\theta_s) \delta[t - \tau_{n,m}(\theta_s)] \quad (3)$$

where the $\{a_{n,m}(\theta_s), \tau_{n,m}(\theta_s); n = 1, \dots, N; m = 1, \dots, M\}$ are, respectively, the signal attenuations and time delays along the M acoustic paths at time snapshots $n = 1, \dots, N$.

To proceed with the estimation of the $\tau_{n,m}; m = 1, \dots, M; n = 1, \dots, N$ time delays, it is necessary to assume that the variation in time delays is small within each N snapshot data set, i.e., that $\tau_{n,m} = \tau_m + \delta\tau_{n,m}$ where $\delta\tau_{n,m} \ll \tau_m$ and $\delta\tau_{n,m} \ll T_0$ where T_0 is the observation time ($T_0 = NT\Delta t$, where Δt is the sampling interval). This additional assumption allows one to write

$$z_n(t, \theta_s) = \sum_{m=1}^M a_{n,m}(\theta_s) s_0[t - \tau_m(\theta_s)] \quad (4)$$

where $\tau_m(\theta_s)$ is the mean arrival time of path m within the observation time T_0 . With the assumptions made in (4), one can now rewrite (1) as

$$\mathbf{y}_n(\theta_s) = \mathbf{S}[\boldsymbol{\tau}(\theta_s)] \mathbf{a}_n(\theta_s) + \epsilon_n \quad (5)$$

with the following matrix notations:

$$\mathbf{y}_n(\theta_s) = [y_n(1, \theta_s), y_n(2, \theta_s), \dots, y_n(T, \theta_s)]^t, \quad \dim T \times 1 \quad (6a)$$

$$\boldsymbol{\tau}(\theta_s) = [\tau_1(\theta_s), \dots, \tau_M(\theta_s)]^t, \quad \dim M \times 1 \quad (6b)$$

$$\mathbf{s}_0(\tau) = [s_0(-\tau), \dots, s_0((T-1)\Delta t - \tau)]^t, \quad \dim T \times 1 \quad (6c)$$

$$\mathbf{S}[\boldsymbol{\tau}(\theta_s)] = [\mathbf{s}_0(\tau_1), \dots, \mathbf{s}_0(\tau_M)], \quad \dim T \times M \quad (6d)$$

and

$$\mathbf{a}_n(\theta_s) = [a_{n,1}(\theta_s), \dots, a_{n,M}(\theta_s)]^t, \quad \dim M \times 1 \quad (6e)$$

where T is the number of time samples on each snapshot and M is the number of signal replicas at the receiver. Equation (5) forms a linear model on the amplitude vector \mathbf{a} , where further assumptions on the relative dimensions and rank of matrix \mathbf{S} and noise distributions allow for different solutions for the estimation of $\boldsymbol{\tau}$. For simplicity, the dependence of $\boldsymbol{\tau}$ and \mathbf{a} on the source location parameter θ_s will be omitted in the next two sections.

III. TIME DELAY AND AMPLITUDE ESTIMATORS

In model (5), both the amplitude and the time-delay vectors are unknown. However, as discussed in the introduction, we prefer to focus on the time-delay vector for localization which should be a more stable feature and therefore yield a more robust processor. There are two possible approaches for solving this problem: the first is to consider that the amplitude vector is deterministic and therefore both \mathbf{a} and $\boldsymbol{\tau}$ are to be estimated; the second considers that \mathbf{a} can also be random, and then one has to resort to second-order statistics for estimating the time-delay vector $\boldsymbol{\tau}$. These two approaches will be formulated in the next subsections.

A. Deterministic Amplitudes

To begin, one needs some estimate of the amplitude vector \mathbf{a} . This is a classical problem and may be easily addressed using the least squares (LS) method or, under the Gaussian white noise assumption, treated as a generalized maximum likelihood (ML) problem. In either case, one obtains the following:

$$\hat{\mathbf{a}} = \arg \left\{ \min_{\mathbf{a}} c(\boldsymbol{\tau}, \mathbf{a}) = \|\mathbf{y} - \mathbf{S}(\boldsymbol{\tau})\mathbf{a}\|^2 \right\} \quad (7)$$

whose solution is well known as

$$\hat{\mathbf{a}} = (\mathbf{S}^H \mathbf{S})^{-1} \mathbf{S}^H \mathbf{y} \quad (8)$$

where H indicates complex conjugate transpose. Inserting $\hat{\mathbf{a}}$ of (8) into (5), the problem now becomes that of estimating a known signal in white noise (for each assumed $\boldsymbol{\tau}$). The optimal solution is given by the well-known matched filter. That can be seen by inserting (8) into (7) to obtain a new function to be maximized

$$c(\boldsymbol{\tau}) = \|\mathbf{y}^H \mathbf{S}(\boldsymbol{\tau})\|^2 \quad (9)$$

which is now only a function of delay vector $\boldsymbol{\tau}$. Passing from (7) to (9), requires the additional assumption that the matrix \mathbf{S} is orthogonal, i.e., that $\mathbf{S}^H \mathbf{S} = \mathbf{I}$. In terms of propagation, that assumption is equivalent to assuming that signals traveling along different paths suffer uncorrelated perturbations. Whether this occurs in practice depends on a variety of factors.

The description above assumes that only a single measurement \mathbf{y} is available. If, instead, there are N randomly distributed vectors inserted into a matrix as $\mathbf{Y} = [\mathbf{y}_1, \dots, \mathbf{y}_N]$, of dimension $T \times N$, the problem is formulated as the minimization of

$$\|\mathbf{Y} - \mathbf{S}(\tau)\mathbf{A}\|^2 \quad (10)$$

where \mathbf{A} is now a $M \times N$ matrix containing the M signal amplitudes at N times. In this case, the solution for \mathbf{A} is analogous to (8) as

$$\hat{\mathbf{A}} = (\mathbf{S}^H \mathbf{S})^{-1} \mathbf{S}^H \mathbf{Y}. \quad (11)$$

Substituting (11) into (10) gives the new function for τ as

$$e(\tau) = \frac{1}{N} \sum_{n=1}^N \|\mathbf{y}_n^H \mathbf{S}(\tau)\|^2. \quad (12)$$

In this case, and for an infinite observation time, one can estimate the M time delays from the M highest peaks of function (12), i.e.,

$$\{\hat{\tau}_m^{\text{LS}}; m = 1, \dots, M\} = \arg \left\{ \max_{\tau} \sum_{n=1}^N \|\mathbf{y}_n^H \mathbf{s}_0(\tau)\|^2 \right\} \quad (13)$$

and then replace the time-delay estimates obtained from (13) into matrix \mathbf{S} of the amplitude estimator (11) and iterate. In practice, for a finite observation time, (12) may not exhibit M clear peaks, and a complex M -dimensional search may be required to solve (13). As it will be seen below, such a complex search procedure is not needed here since only the value of the functional (12), at model predicted values of τ , is necessary for source localization.

B. Random Amplitudes

Once model (5) has been adopted, an additional assumption on the mutual decorrelation of the multipath amplitudes (assumed now as random and zero mean) allows one to extend the least squares or maximum likelihood (LS/ML) method above to subspace separation-based methods.² In fact, the linear model (5) allows one to characterize the signal part as covering a $K (< M)$ -dimensional subspace where K is the number of uncorrelated paths (or groups of paths) in the received signal—this is the signal subspace.

In general, a number $N \geq M$ of uncorrelated time snapshots are available which is a requirement for estimating the signal subspace. Let us consider the data matrix \mathbf{Y} and its SVD $\mathbf{Y} = \mathbf{U}\mathbf{\Sigma}\mathbf{V}^H$. Since $T > N$, \mathbf{Y} has a maximum rank of N . Taking into account the linear model (5) with the assumptions made on the decorrelation of noise, signal, and amplitude components, it can be shown [18] that the M eigenvectors $\{\mathbf{u}_1, \dots, \mathbf{u}_M\}$ associated with the M largest singular values $\sigma_1 \geq \sigma_2 \geq \dots \geq \sigma_M$ provide the optimal estimate (in the sense of LS and ML) of the signal subspace. Indeed, the vectors $\mathbf{u}_m; m = 1, \dots, M$ span the same (signal) subspace as the M signal replicas $\mathbf{s}_0(\tau_1), \dots, \mathbf{s}_0(\tau_M)$. Therefore, considered as a function of search delay τ , the projection of the signal replicas onto the subspace spanned by the first M eigenvectors will be

a maximum for $\tau = \tau_m; m = 1, \dots, M$. Thus, we seek the maxima of the functional

$$e(\tau) = \|\mathbf{U}_M^H \mathbf{s}_0(\tau)\|^2 \quad (14)$$

where $\mathbf{U}_M = [\mathbf{u}_1, \dots, \mathbf{u}_M]$. Using (14), the associated signal subspace (SS) based time-delay τ_m estimator can be written as

$$\{\hat{\tau}_m^{\text{SS}}; m = 1, \dots, M\} = \arg \left\{ \max_{\tau} \|\mathbf{U}_M^H \mathbf{s}_0(\tau)\|^2 \right\}. \quad (15)$$

Similarly, knowing that \mathbf{U}_M and its complement $\mathbf{U}_{T-M} = \mathbf{U}_M^\perp$ split the whole space \mathbb{R}^T into two orthogonal subspaces, the projection of the signal replicas onto the \mathbf{U}_M signal subspace complement (denoted SS^\perp in the sequel) will tend to zero for the same true values of τ . Therefore, the noise subspace-based time-delay τ_m estimator is given by

$$\begin{aligned} \{\hat{\tau}_m^{\text{SS}^\perp}; m = 1, \dots, M\} \\ = \arg \left\{ \max_{\tau} \left[\|\mathbf{U}_{T-M}^H \mathbf{s}_0(\tau)\|^2 \right]^{-1} \right\} \end{aligned} \quad (16)$$

where the matrix $\mathbf{U}_{T-M} = [\mathbf{u}_{M+1}, \dots, \mathbf{u}_T]$ is formed from the data eigenvectors associated with the $M + 1$ to T smallest singular values. These eigenvectors span the subspace containing the nonsignal components, so the estimator is generally called the noise subspace or signal subspace orthogonal estimator.

IV. SOURCE LOCALIZATION

The source localization problem can be readily deduced from the last sections both for the LS/ML and the subspace separation-based methods. Until now, only the received signal was used for analysis but source localization requires data inversion for source properties. That means, in particular, that the medium where the signal is propagating has to be taken into account using a specific propagation model to solve the forward problem. The propagation model determines a set of time delays at the receiver for the given environment and for each hypothetical source location.

Let us define $\boldsymbol{\tau}(\theta)$ as the model-calculated time delay vector for source location θ , conditioned on a given environmental scenario. For all possible values of θ in a set Θ , the vector $\boldsymbol{\tau}(\theta)$ will cover a continuum on an M -dimensional space as does the source replica vector. In other words, the source replica vectors span a subspace $S(\theta)$ that has dimension M under the assumption of uncorrelated paths

$$S(\theta) = \text{range}(\mathbf{S}[\boldsymbol{\tau}(\theta)]) = \text{range}\{\mathbf{s}_0[\boldsymbol{\tau}(\theta)]; \theta \in \Theta\}. \quad (17)$$

As explained in the previous section, an estimate of the actual $S(\theta_s)$ subspace associated with the true source location can be obtained as the span of the M eigenvectors contained in \mathbf{U}_M :

$$\hat{S}(\theta_s) = \text{range}(\mathbf{U}_M). \quad (18)$$

Those two subspaces share the same dimension M . An estimator $\hat{\theta}_s$ of θ_s could, in principle, be derived from the notion of distance between subspaces. This is usually based on respective projections, but alternatively one may use the CS decomposition theorem [19, Theorem 2.6.1] and define the distance measure

$$d(\theta) = \sqrt{1 - \sigma_{\min}^2(\mathbf{U}_M^H \mathbf{S}[\boldsymbol{\tau}(\theta)])}, \quad \theta \in \Theta \quad (19)$$

where $\sigma_{\min}(\bullet)$ is the minimum singular value of matrix \bullet . The distance measure (19) demonstrates poor performance for esti-

²Subspace methods do not require random amplitudes that can be either random or deterministic.

imating the source location parameter θ_s , since it mainly depends on the estimation of the smallest eigenvalue of a matrix that is itself highly dependent on the SNR. In practice, M is not known and varies with θ , which introduces further sensitivity into $d(\theta)$.

Alternatively, a constrained LS/ML based estimate $\hat{\theta}_{LS}$ of source location θ_s will be, according to (12) and (13), given by the value of θ that satisfies

$$\max_{\tau(\theta)} \frac{1}{N} \sum_{n=1}^N \|\mathbf{S}[\tau(\theta)]^H \mathbf{y}_n\|^2, \quad \theta \in \Theta. \quad (20)$$

The resulting source location estimator can therefore be written as

$$\hat{\theta}_{LS} = \arg \left\{ \max_{\tau(\theta)} \frac{1}{N} \sum_{n=1}^N \sum_{m=1}^M \|\mathbf{s}_0[\tau_m(\theta)]^H \mathbf{y}_n\|^2 \right\}, \quad \theta \in \Theta. \quad (21)$$

Similarly, using (15) and (21) for the SS approach, the source location estimate corresponds to the maximum of the sum over paths of the projections of the replica signal for each time delay set onto the estimated signal subspace

$$\hat{\theta}_{SS} = \arg \left\{ \max_{\tau(\theta)} \sum_{m=1}^M \|\mathbf{U}_M^H \mathbf{s}_0[\tau_m(\theta)]\|^2 \right\}, \quad \theta \in \Theta. \quad (22)$$

Finally, for the SS^\perp approach, the function is searched for the minimum of the sum over paths of the projections onto the noise subspace estimate

$$\hat{\theta}_{SS^\perp} = \arg \left\{ \min_{\tau(\theta)} \sum_{m=1}^M \|\mathbf{U}_{T-M}^H \mathbf{s}_0[\tau_m(\theta)]\|^2 \right\}, \quad \theta \in \Theta. \quad (23)$$

V. SIMULATION RESULTS

In order to test the methods presented in the previous section, and to have a feeling of their performance on real data, the environmental and geometry scenario used for simulation was the same as that of the real data in the next section. Let us consider the case of an LFM sweep with a duration $D_t = 1$ s and a frequency band from 200 to 400 Hz. The signal is transmitted in a 135-m-deep waveguide with a slightly downward refracting sound speed profile (Table I) over a sandy bottom characterized by a 1750-m/s sound speed, a density of 1.9 g/cm³, and a compressional attenuation of 0.8 dB/ λ (Fig. 1). The ray-arrival times and amplitudes predicted with Bellhop [20] for a sound source and a receiver at depths of 92 and 115 m, respectively, 5.6 km away from each other, are shown in Fig. 2. The arrivals are arbitrarily ordered in accordance with their takeoff angle at the source. The intermediate angles correspond to rays which are launched nearly horizontally, therefore, with smaller amplitude loss as seen in Fig. 2(a). Their path lengths are shortened, yielding a bowl-shaped arrival time pattern seen in Fig. 2(b).

A number of $N = 100$ snapshots were generated according to model (5) with a high SNR (>20 dB), and the decorrelation between multipath amplitudes was simulated by generating a Gaussian vector with its mean equal to the value given by the model [Fig. 2(a)], and its standard deviation $\sigma_a = 0.5\|\mathbf{a}\|$. The corresponding arrival pattern, based on (13), is shown in Fig. 3. Note that there are many more arrivals in Fig. 2 than we

TABLE I
MEASURED SOUND SPEED PROFILE USED IN THE SIMULATION EXAMPLE

Depth (m)	Sound speed (m/s)
0.0	1520
5.0	1520
11.3	1518
21.3	1516
32.0	1512
42.7	1510
72.8	1508
94.6	1507
135.0	1507

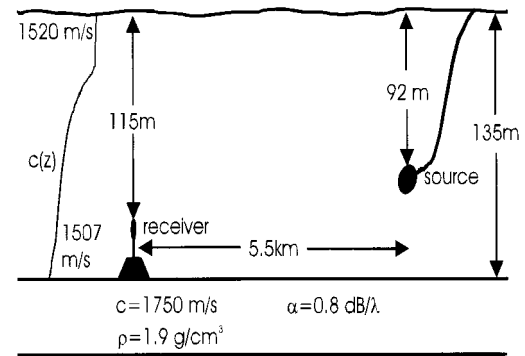


Fig. 1. INTIMATE'96 real data environmental scenario used for the simulation.

see as peaks in Fig. 3. This indicates that there are many unresolved paths. (With increased bandwidth, these paths would be resolved.)

Fig. 4 shows the arrival pattern for the same data set but using the signal subspace estimator (15) with the number of arrivals set to the true number, i.e., $M = 48$. Notice that the higher resolution allows one to distinguish many more arrivals. The amplitudes are not proportional to the received signal correlation since no eigenvalue weighting was used to project the source signal onto the signal subspace. Fig. 5 shows the arrival pattern obtained with the noise subspace estimator (16). The path resolution is the same as that of the signal subspace method. However, it is much less sensitive to the actual subspace dimensionality since an underestimation of M would result in a misprojection onto the signal subspace. Numerically, this is a large number and therefore a small contribution to the inverse function in the noise subspace estimator. On the other hand, an overestimation of M would result in a few unobserved directions among several thousand (depending on the value of T) which, in practice, has little effect on the result. The main practical difficulty is simply the computational cost of manipulating matrices of high dimension. For that reason, the estimators were implemented in the frequency domain for the real data analysis of the next section.

VI. REAL DATA ANALYSIS

The INTIMATE'96 sea trial was primarily designed as an acoustic tomography experiment to observe internal tides and details of the experimental setup has appeared elsewhere [21]. However, for the sake of completeness, a brief description of

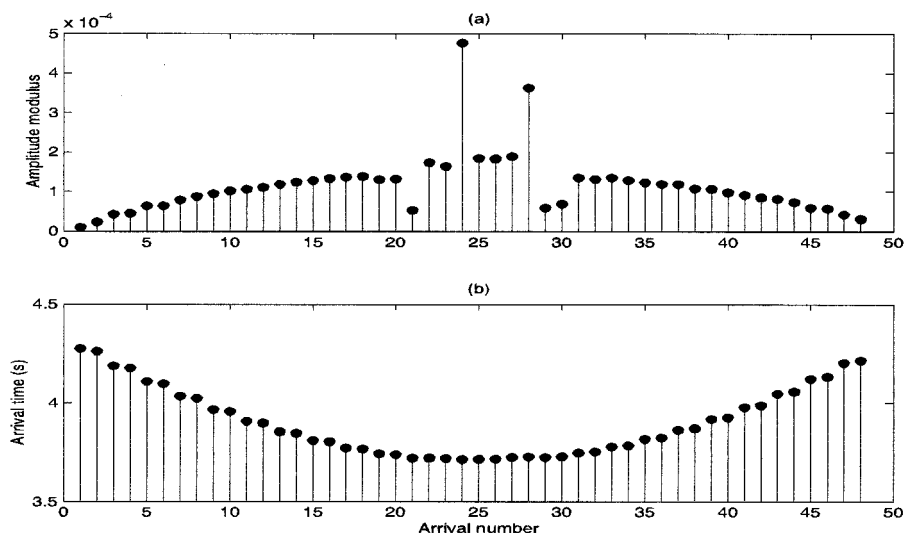


Fig. 2. Ray-model predicted arrival (a) amplitudes and (b) times.

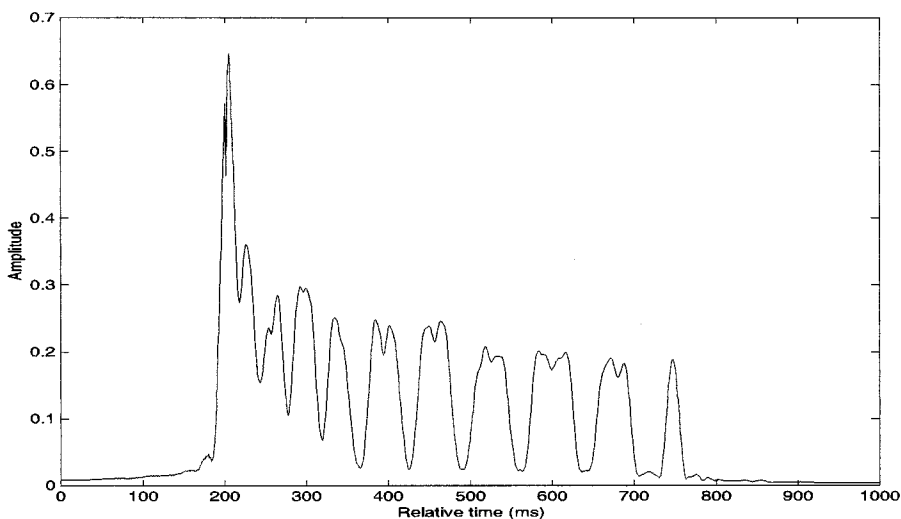


Fig. 3. Arrival pattern with LS/ML estimator [see (13)].

the experiment follows. The experiment was conducted in the continental platform near the town of Nazaré, off the west coast of Portugal, during June 1996 and consisted of several phases during which the acoustic source was either stationary or being towed along predetermined paths. This paper is concerned with the data acquired in phase 1 during which the scenario is as shown in Fig. 1 and is identical to that used for the simulations in Section V. The only difference is that the source signal used during INTIMATE'96 was a 300–800-Hz LFM sweep with 2-s duration repeated every 8 s. The signal received at 5.5-km range on the 115-m-depth hydrophone is shown in Fig. 6. At that range, the time–frequency source signature could be clearly seen [Fig. 6(a)], while the time series shows a strong multipath effect [Fig. 6(b)]. The SNR has been estimated to be approximately 10 dB within the frequency band of interest. As a first test of the match between the predicted arrival times and the estimated arrival patterns, Fig. 7 shows an example of a received data arrival pattern using (13). The corresponding predicted arrival times are represented by the vertical lines on the time axis. The

agreement between the two patterns is almost perfect for this case. In order to establish a localization statistic, the algorithms described above were used to estimate the source range at a given correct source depth. Separately, we have estimated the source depth using a given (correct) range during a 20-h run (phase 1) where the source was held at approximately a constant range and depth and the environment was nearly range-independent with a 135-m-depth channel and a slightly downward refracting sound speed (as explained in Section V and in detail in [21]).

The first problem encountered when processing the real data using the subspace-based methods was the estimation of the number of existing paths M in (22) and (23). In principle, M can be predicted by the acoustic model for each source range and should be equal to the rank of matrix \mathbf{S} . However, in practice, it was found that the matrix \mathbf{S} was largely rank deficient, and the number of estimated uncorrelated paths (or path groups) was much smaller than the number of predicted paths M . Fig. 8 shows the number of estimated paths for a 20-h run using the classical Akaike Information Criterion (AIC) and Minimum Description

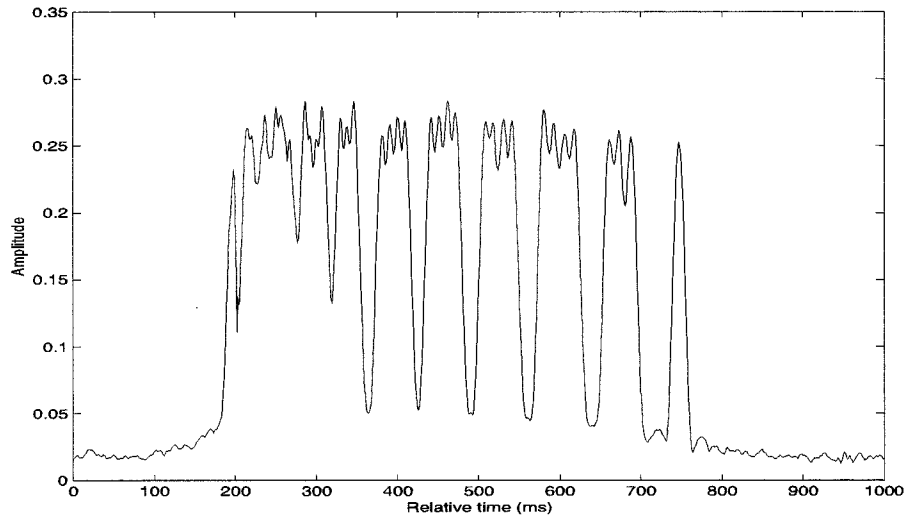


Fig. 4. Arrival pattern with an SS estimator [see (15)] and $M = 48$.

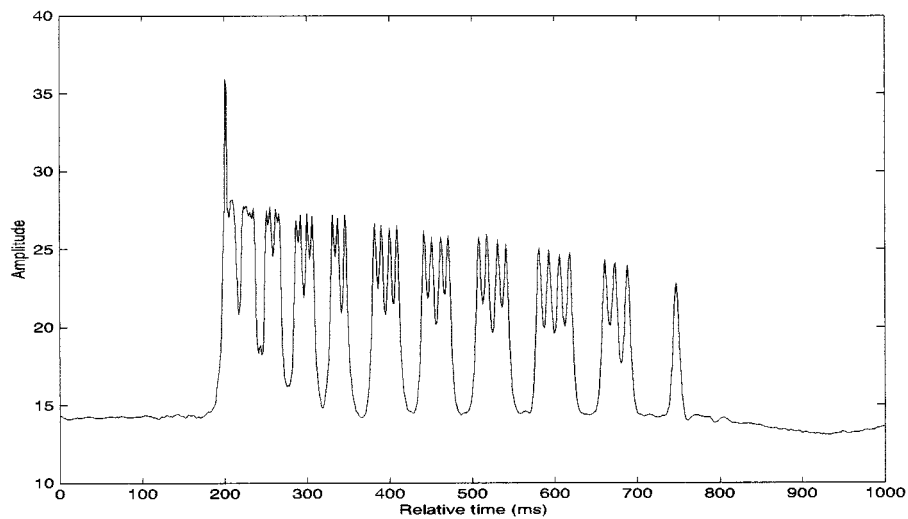


Fig. 5. Arrival pattern with a SS^\perp estimator [see (16)] and $M = 48$.

Length (MDL) [22]. It can be seen in Fig. 8 that the estimated number of paths varies from 4 to 5 for AIC and from 3 to 4 for MDL (while the model predicted number of paths is $M = 48$).

It is known that AIC tends to give higher estimates than MDL and, in many practical situations, to overestimate the model order so these results are anticipated. In our case, the AIC and MDL order estimates inserted into (22) and (23) yield approximately the same results, so we will only present the former. In Fig. 9, we estimated source range and in Fig. 10 we estimated source depth. In these figures, the three estimators (21), (22), and (23) are, respectively, shown in ambiguity plots (a), (b), and (c). Taking the peak locations from those plots yields corresponding subplots (d), (e), and (f), showing the estimated location (either range or depth) versus time. A statistic of the estimated mean and MSE of the proposed estimators is summarized in Table II. The data singular-value decomposition was performed on 35 consecutive data snapshots every 5 min, with each snapshot containing a single received source waveform. Therefore, the data shown has 231 samples along the time axis and, since the

samples are 5 min apart, the whole data set represents 19.25 h worth of data. Fig. 9(a) and (b), given by the LS/ML and SS estimators, are very similar and show a relatively stable and well-defined estimate with a mean source range of 5.48 km (Figs. 9(d) and (e) and Table II), which coincides with the mean DGPS range estimate recorded during the cruise. The waving effect seen in time is mainly due to the surface tide (Fig. 11). The phase coincidence between tide height and the range estimate is striking and simply shows the influence of water depth variation on the multipath time-delay structure between the source and the receiver. Fig. 9(c), obtained with the signal subspace orthogonal projector, shows a more ambiguous surface—larger mean square error (MSE)—with, however, the same mean source range estimate than for the other estimators (Fig. 9(f) and Table II). This poorer result is possibly due to the signal subspace rank deficiency mentioned above. The first impression from Fig. 10, when compared to Fig. 9, is that the results are poorer for source depth than for source range. This is mainly a function of the axis scales since we localize in range over a wide sweep while depths

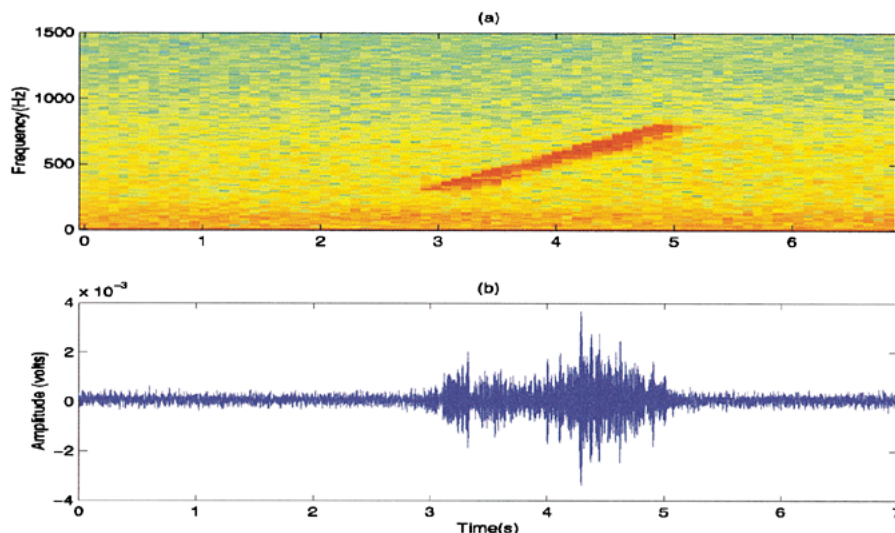


Fig. 6. Received signal at 115-m depth and 5.5 km range: (a) time–frequency plot and (b) time series.

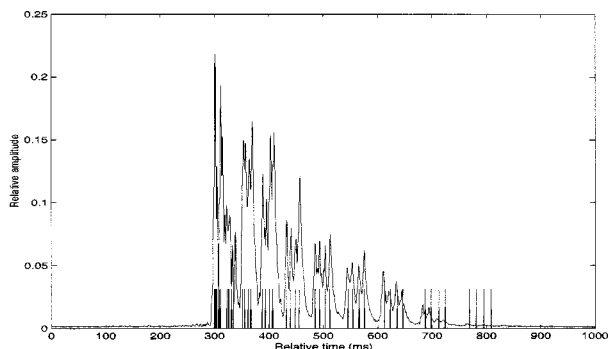


Fig. 7. Arrival pattern using the LS estimator for a sound source at 5.5-km range and 92-m depth received on a sensor at 115-m depth. Vertical lines on the time axis represent Bellhop-predicted arrival times.

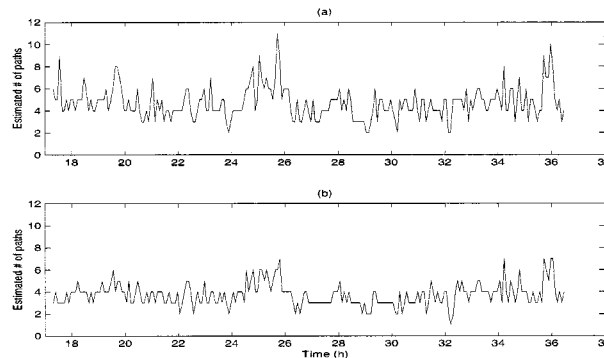


Fig. 8. Estimated number of uncorrelated paths with (a) AIC criterion and (b) the MDL criterion. The start time is 17:20, June 14, 1996.

of interest are limited to the channel depth. There is also a dependence on the basic variation of the acoustic field; however, in terms of intensity, the characteristic scale is a few wavelengths in both range and depth. Among the three estimators shown in Fig. 10(a)–(c) is the signal subspace that provided the best mean result with 92 m, very close to the true nominal value and also the lowest estimated MSE. However, all the methods perform well and there is little practical basis for choosing one over the other. The authors also believe that, if a broad-band random source signal was used, the results would be similar to those obtained with the LFM deterministic signals provided that the emitted signal replicas were known at the receiver and that the frequency band was identical.

VII. DISCUSSION AND CONCLUSIONS

The discussion of the results can be separated into two distinct aspects: one is the estimation of the arrival times—which is a question of time-delay estimation—and the other is the usage of the estimated pattern to match the predicted arrival times and its impact on source localization. Time-delay estimation has been intensively studied in the underwater acoustic multipath context

(see, for example, [23]–[26] and references therein). Three different methods were presented here only to emphasize the importance of the high resolution of time delays in the presence of limited bandwidth signals. The source localization aspect is much more central to the paper and, in that respect, the results shown should be compared with those obtained by Porter *et al.* [15], [16], in which a method similar to (21) is used but the correlation is made between the log of the received signal and the log of the predicted arrival signal. The output is the peak of the correlation function. The motivation for that processor is discussed more extensively in those papers. Briefly, the log processor brings into balance the strong early arrivals with the weak late arrivals. The resulting estimator accentuates the basic arrival pattern (in terms of arrival times) rather than the arrival amplitude. However, as the processor is based on a correlation of the complete time-series, it is sensitive to both the peaks and valleys of the data. In the present study, even greater emphasis is placed on the arrival times of the individual paths. In fact, the match function given by (21) is made only for the predicted arrival times. In other words, only the peaks of the arrival pattern (assuming the correct prediction of time delays) are used. Obviously, the result will be optimal if the peak locations are correctly predicted and resolved, and this is why subspace methods

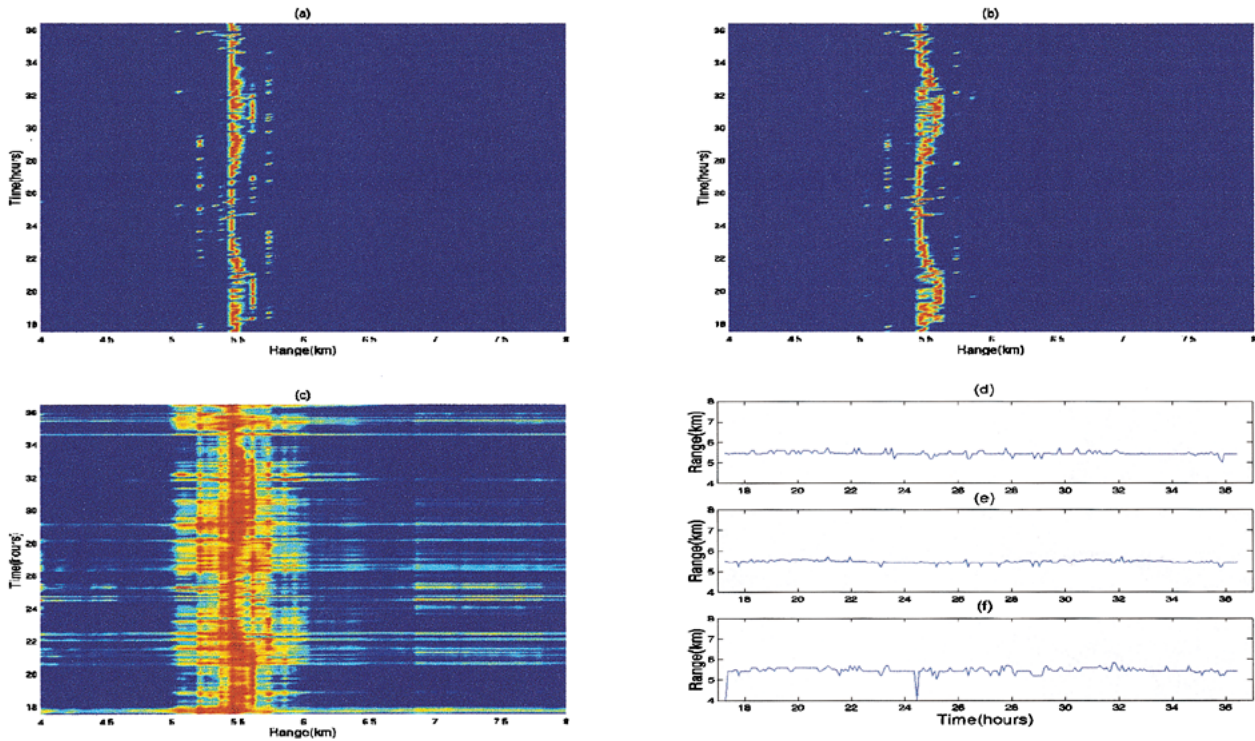


Fig. 9. Time-range localization plots for INTIMATE'96 phase 1 data set with (a) LS/ML method, (b) signal subspace, and (c) noise subspace projection. (d)–(f) The range estimate obtained as the max on each surface (a)–(c), respectively. The start time is 17:20, June 14, 1996.

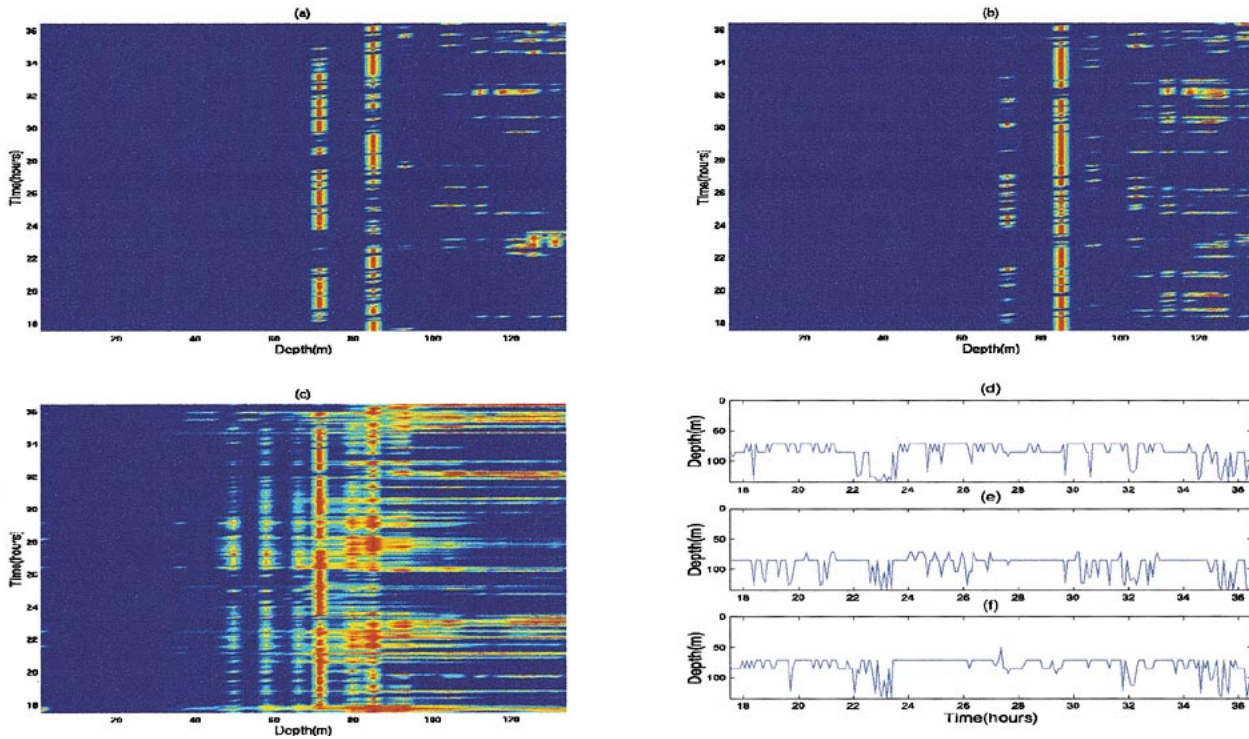


Fig. 10. Time-depth localization plots for INTIMATE'96 phase 1 data set with (a) LS/ML method, (b) signal subspace, and (c) noise subspace projection. (d)–(f) The depth estimate obtained as the max on each surface (a)–(c), respectively. The start time is 17:20, June 14, 1996.

have been introduced for time-delay resolution enhancement. Conversely, errors on the prediction of arrival times would directly impact on the quality of the localization. In terms of the required computation effort, the methods presented here gen-

erally take approximately five times the computation time than that required by Porter's method under the same conditions.

This paper has presented a comprehensive method for source localization using broad-band signals received on a single hy-

TABLE II
SOURCE LOCALIZATION IN RANGE AND DEPTH: ESTIMATED MEAN AND MEAN SQUARE ERROR (MSE) FOR THE THREE METHODS: LS/ML, SS AND SS[⊥]

	Range (m)		Depth (m)	
	mean	mse	mean	mse
LS/ML	5.48	9.3	85	348
SS	5.49	7.1	92	259
SS [⊥]	5.48	34.7	80	363

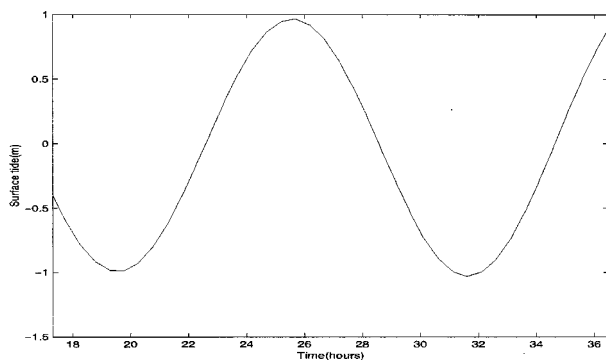


Fig. 11. Surface tide prediction for the receiver location. The start time is 17:20, June 14, 1996.

drophone. The method assumes a classical model of the received data as a linear combination of time-delayed replicas of the emitted waveform with unknown but uncorrelated random amplitudes. The received signal is assumed to be corrupted by white Gaussian noise and in all cases the emitted signal is supposed to be known at the receiver. First, classical TDE methods for estimating the time-delay set are presented and tested on simulated data. Then subspace-based methods are obtained, in a classical way, for estimating the signal subspace spanned by the received paths and its orthogonal complement.

It is shown that time delays can be derived from the intersection of the signal subspace estimate and the subspace spanned by the replica signals. For computing the replica signals, there are now a variety of well-developed acoustic models suitable for this application including normal mode, PE, wavenumber integration, and ray models. Ray models have a clear speed advantage for these broad-band applications since the ray approximation produces broad-band information (arrival times and amplitudes) for no additional cost. Of course, ray models are also generally the least accurate; however, they were found fully adequate for our application.

The source location estimators are then computed as the sum of the contributions of the match between the received and replica signals at the predicted arrival times. The match itself is performed in three different ways using: 1) the full received signal; 2) the projection of the received signal onto the signal subspace; and 3) its complement projection onto the noise subspace.

These source location estimators have been applied to localize a sound source emitting a 300–800-Hz, 2-s-long LFM sweep recorded in a shallow water area off the coast of Portugal. The source range or depth have been successfully tracked during a 20-h time period. The results obtained show the feasibility of single sensor source localization at a known depth

or at a known range: source range can be estimated within a few meters from the true range of 5.5 km, while, for source depth, the results show some persistent biases and estimation errors varying between a few meters up to several tens of meters from the expected true source depth of 92 m. Comparison of the methods presented here with the results obtained in the same data set by Porter *et al.* [15], [16] show that rather different approaches gave very similar results with, however, a significant advantage in terms of computer time requirements for the latter. The methods presented here, in particular those that are subspace-based, should have an advantage relative to that of Porter when the signal has a narrower band that only allows for a few paths to be resolved at the receiver. The results obtained with real data show that the correlation and interaction between acoustic paths plays an important role in source localization giving new insights into the understanding of how their combination and (re)combination forms complex arrival patterns.

ACKNOWLEDGMENT

The authors acknowledge the support of SACLANTCEN for lending the acoustic receiving system and the dedicated collaboration of P. Felisberto in the real data acquisition and processing during INTIMATE'96.

REFERENCES

- [1] M. J. Hinich, "Maximum-likelihood signal processing for a vertical array," *J. Acoust. Soc. Amer.*, vol. 54, pp. 499–503, 1973.
- [2] H. P. Bucker, "Use of calculated sound fields and matched-field detection to locate sound sources in shallow water," *J. Acoust. Soc. Amer.*, vol. 59, pp. 368–373, 1976.
- [3] A. B. Baggeroer and W. A. Kuperman, "Matched field processing in underwater acoustics," in *Proc. NATO ASI Conf. on Acoustic Signal Processing for Ocean Exploration*, Madeira, Portugal, 1992, pp. 83–122.
- [4] A. B. Baggeroer, W. A. Kuperman, and H. Schmidt, "Matched-field processing: Source localization in correlated noise as an optimum parameter estimation problem," *J. Acoust. Soc. Amer.*, vol. 83, pp. 571–587, 1988.
- [5] S. M. Jesus, "Broadband matched-field processing of transient signals in shallow water," *J. Acoust. Soc. Amer.*, pt. 1, vol. 93, no. 4, pp. 1841–1850, 1993.
- [6] S. P. Czenszak and J. L. Krolik, "Robust wideband matched-field processing with a short vertical array," *J. Acoust. Soc. Amer.*, vol. 101, no. 2, pp. 749–759, 1997.
- [7] C. S. Clay, "Optimum time domain signal transmission and source location in a waveguide," *J. Acoust. Soc. Amer.*, vol. 81, 1987.
- [8] A. Parvulescu and C. S. Clay, "Reproducibility of signal transmissions in the ocean," *Radio Eng. Electron.*, vol. 29, pp. 223–228, 1965.
- [9] S. Li and C. S. Clay, "Optimum time domain signal transmission and source location in a waveguide: Experiments in an ideal wedge waveguide," *J. Acoust. Soc. Amer.*, vol. 82, no. 4, pp. 1409–1417, 1987.
- [10] L. N. Frazer and P. I. Pecholcs, "Single-hydrophone localization," *J. Acoust. Soc. Amer.*, vol. 88, no. 2, pp. 995–1002, 1990.
- [11] J. H. Miller and C. S. Chiu, "Localization of the sources of short duration acoustic signals," *J. Acoust. Soc. Amer.*, vol. 92, no. 5, pp. 2997–2999, 1992.
- [12] D. P. Knobles and S. K. Mitchell, "Broadband localization by matched fields in range and bearing in shallow water," *J. Acoust. Soc. Amer.*, vol. 96, no. 3, pp. 1813–1820, 1994.
- [13] R. K. Brienza and W. Hodgkiss, "Broadband matched-field processing," *J. Acoust. Soc. Amer.*, vol. 94, no. 5, pp. 2821–2831, 1993.
- [14] G. C. Carter, "Variance bounds for passively locating an acoustic source with a symmetric line array," *J. Acoust. Soc. Amer.*, vol. 62, no. 4, pp. 922–926, 1977.
- [15] M. B. Porter, S. Jesus, Y. Stéphan, X. Démoulin, and E. Coelho, "Exploiting reliable features of the ocean channel response," in *Proc. SWAC'97*, Beijing, China, Apr. 1997.
- [16] M. B. Porter, Y. Stéphan, X. Démoulin, S. Jesus, and E. Coelho, "Shallow-water tracking in the sea of Nazaré," in *Proc. Underwater Technologies '98*, Tokyo, Japan, 1998.

- [17] W. Munk, P. Worcester, and C. Wunsch, *Ocean Acoustic Tomography*. Cambridge, U.K.: Cambridge University Press, 1995.
- [18] O. R. Schmidt, "A signal subspace approach to multiple emitter location and spectral estimation," Ph.D. dissertation, Stanford Univ., Stanford, CA, 1982.
- [19] G. Golub and C. Van Loan, *Matrix Computations*, 2nd ed. Baltimore, MD: The John Hopkins Press, 1989, pp. 77–78.
- [20] M. B. Porter and Y. C. Liu, "Finite-element ray tracing," in *Proc. Int. Conf. on Theoretical Comp. Acoust.*, vol. 2, D. Lee and M. H. Schultz, Eds, Singapore, 1993, pp. 947–956.
- [21] X. Démoulin, Y. Stéphan, S. Jesus, E. Coelho, and M. B. Porter, "INTIMATE96: A shallow water tomography experiment devoted to the study of internal tides," in *Proc. SWAC'97*, Beijing, China, Apr. 1997.
- [22] M. Wax and T. Kailath, "Detection of signals by information theoretic criteria," *IEEE Trans. Acoust., Speech, Signal Processing*, vol. ASSP-33, pp. 387–392, 1985.
- [23] C. H. Knapp and G. C. Carter, "The generalized correlation method for estimation of time delay," *IEEE Trans. Acoust., Speech, Signal Processing*, vol. ASSP-24, pp. 320–327, 1976.
- [24] Y. T. Chan, R. V. Hattin, and J. B. Plant, "The least squares estimation of time delay and its use in signal detection," *IEEE Tran. Acoust., Speech, Signal Processing*, vol. ASSP-26, pp. 217–222, 1978.
- [25] J. P. Ianniello, "Time delay estimation via cross-correlation in the presence of large estimation errors," *IEEE Trans. Acoust., Speech, Signal Processing*, vol. ASSP-30, pp. 998–1003, 1982.
- [26] J. C. Rosenberger, "Passive localization," in *Proc. NATO ASI on Underwater Acoustics Data Processing*, 1989, pp. 511–524.



Sérgio M. Jesus (A'93) received the "Doctorat Es-Sciences" degree in engineering sciences from the Université de Nice, France, in 1986.

From 1986 to 1992, he was a Staff Scientist at the SACLANT Undersea Research Centre, La Spezia, Italy, in the Ambient Noise and Signal Processing Groups. During that period, he was involved with underwater acoustic field noise directionality and early studies on target detection using matched field processing. In 1992, he joined the Electrical Engineering and Computer Department at the University

of Algarve, Faro, Portugal, where he is currently Associate Professor. His interests are underwater acoustics signal processing, model-based inversion, ocean and seafloor tomography, and underwater communications.

Dr. Jesus is a member of EURASIP and the Acoustical Society of America.

Michael B. Porter was born in Quebec, Canada, on September 19, 1958. He received the B.S. degree in applied mathematics from the California Institute of Technology, Pasadena, in 1979 and the Ph.D. degree in engineering science and applied mathematics from Northwestern University, Evanston, IL, in 1984.

From 1983 to 1985, he was a Scientist at the Naval Ocean Systems Center, San Diego, CA, where he performed research in numerical modeling of antennas, optical fibers, sonar transducers, and ocean acoustics problems. From 1985 to 1987, he was employed as a Research Physicist at the Naval Research Laboratory (NRL) in Washington, DC. At NRL, his interest included matched-field processing and computational acoustics. From 1987 to 1991, he continued research in these areas as a Senior Scientist at the SACLANT Undersea Research Centre (NATO) in La Spezia, Italy. For the last nine years, he has been with the Department of Mathematical Sciences at the New Jersey Institute of Technology as Associate then Full Professor. During this time, he also held visiting positions at the University of Algarve and the Scripps Institution of Oceanography. He is presently on leave from the New Jersey Institute of Technology, Newark, at SAIC, where he is an Assistant Vice President with the Ocean Sciences Division.

Dr. Porter is the recipient of the A. B. Wood Medal from the Institute of Acoustics and an Innovators Award from the Naval Research Laboratory. He is a fellow of the Acoustical Society of America.



include inverse methods, internal waves tomography, and tactical use of the environment.

Xavier Démoulin received the Magistere of matter sciences from ENSL, Lyon, France, and the D.E.A. degree in physical methods in remote sensing, Paris, France, in 1990.

After receiving his degree, he was employed as a Physicist for several companies. Since 1995, he has been working as an Engineer with the Service Hydrographique et Océanographique de la Marine, Brest, France. His current work is focused on geoacoustics and shallow-water underwater acoustics.



Orlando C. Rodríguez received the Engineer degree in physics from Lomonosov State University, Moscow, Russia, in 1992 and the M.Sc. degree from the University of Algarve, Faro, Portugal. He is currently working toward the Ph.D. degree in acoustic tomography, applied to the detection and inversion of internal tides, at the same university.

In 1992, he was hired as a Teaching Assistant with the Physics Department, University of Algarve. His main interests are acoustic modeling through ray-tracing techniques, internal tides, internal solitary waves, and travel-time-based tomography.

Emanuel M. M. Ferreira Coelho was born in March 1961. He received the M.Sc. and Ph.D. degrees, both in physical oceanography, with a minor in digital signal processing, from the Naval Postgraduate School, Monterey, CA, in 1991 and 1994, respectively.

He is a Hydrographic Engineer with the Portuguese Navy and an Associate Professor with the University Lusófona, Lisboa, Portugal. He is now a Researcher and the Head of the Oceanography Division at the Instituto Hidrográfico, Lisboa, Portugal. His past and present topics of research have covered coordination and participation in several oceanographic campaigns and studies dedicated to mesoscale and submesoscale processes, mainly related to submarine canyons dynamics, quasi-inertial internal waves, and the occurrence of internal dynamical instabilities, development of software for the processing of acoustic data for ocean turbulence measurements in prototype instrumentation, coordination and participation in cruises using both ship-based observations and ROV data for the evaluation of diffusive processes in the upper ocean and for testing of acoustic methods for sea observation, namely acoustic tomography, analysis of near-inertial internal wave propagation over irregular (finite) topography, and nonlinear internal wave generation and propagation.